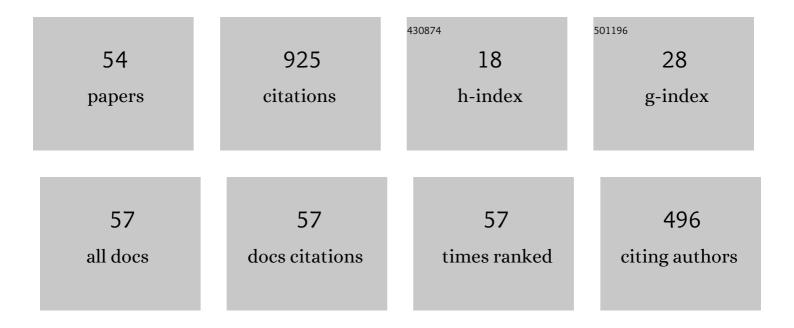
Muhammad Ajmal Khan

List of Publications by Year in descending order

Source: https://exaly.com/author-pdf/4871559/publications.pdf Version: 2024-02-01



#	Article	IF	CITATIONS
1	Highly Transparent pâ€AlGaNâ€Based (326–341 nm)â€Band Ultravioletâ€A Lightâ€Emitting Diodes on AlN Templates: Recent Advances and Perspectives. Physica Status Solidi (A) Applications and Materials Science, 2022, 219, .	1.8	2
2	Achieving 9.6% efficiency in 304Ânm p-AlGaN UVB LED via increasing the holes injection and light reflectance. Scientific Reports, 2022, 12, 2591.	3.3	38
3	Performance enhancement of AlGaN deep-ultraviolet laser diode using compositional Al-grading of Si-doped layers. Optics and Laser Technology, 2022, 152, 108156.	4.6	21
4	Improving AlGaN-based ultraviolet-C (UV–C) light-emitting diodes by introducing quaternary-graded AllnGaN final quantum barrier. Optical Materials, 2021, 112, 110745.	3.6	13
5	Suppressing the efficiency droop in AlGaN-based UVB LEDs. Nanotechnology, 2021, 32, 215703.	2.6	29
6	Impact of Mg level on lattice relaxation in a p-AlGaN hole source layer and attempting excimer laser annealing on p-AlGaN HSL of UVB emitters. Nanotechnology, 2021, 32, 055702.	2.6	23
7	Polarization-dependent hole generation in 222 nm-band AlGaN-based Far-UVC LED: a way forward to the epi-growers of MBE and MOCVD. Journal of Materials Chemistry C, 2021, 9, 16545-16557.	5.5	11
8	Evaluation of internal quantum efficiency and stimulated emission characteristics in AlGaN-based multiple quantum wells. Japanese Journal of Applied Physics, 2021, 60, 120503.	1.5	6
9	Progress on pure AlGaN based UVB LEDs and Our Approach Toward Deep-Ultraviolet (DUV) LDs. , 2021, , \cdot		0
10	Overcoming the current injection issue in the 310Ânm band AlGaN UVB light-emitting diode. Japanese Journal of Applied Physics, 2020, 59, SAAD01.	1.5	19
11	High internal quantum efficiency and optically pumped stimulated emission in AlGaN-based UV-C multiple quantum wells. Applied Physics Letters, 2020, 117, .	3.3	28
12	Correlation between excitons recombination dynamics and internal quantum efficiency of AlGaN-based UV-A multiple quantum wells. Journal of Applied Physics, 2020, 128, .	2.5	23
13	External Quantum Efficiency of 6.5% at 300 nm Emission and 4.7% at 310 nm Emission on Bare Wafer of AlGaN-Based UVB LEDs. ACS Applied Electronic Materials, 2020, 2, 1892-1907.	4.3	45
14	Beyond 53% internal quantum efficiency in a AlGaN quantum well at 326  nm UVA emission and single-peak operation of UVA LED. Optics Letters, 2020, 45, 495.	3.3	26
15	Beyond 53% internal quantum efficiency in a AlGaN quantum well at 326  nm UVA emission and single-peak operation of UVA LED: publisher's note. Optics Letters, 2020, 45, 2563.	3.3	7
16	Influence of Undopedâ€AlGaN Final Barrier of MQWs on the Performance of Lateralâ€Type UVB LEDs. Physica Status Solidi (A) Applications and Materials Science, 2019, 216, 1900185.	1.8	25
17	13 mW operation of a 295–310 nm AlGaN UV-B LED with a p-AlGaN transparent contact layer for real world applications. Journal of Materials Chemistry C, 2019, 7, 143-152.	5.5	84
18	Milliwatt power UV-A LEDs developed by using n-AlGaN superlattice buffer layers grown on AlN templates. Journal Physics D: Applied Physics, 2019, 52, 115102.	2.8	21

#	Article	IF	CITATIONS
19	Improved external quantum efficiency of 293 nm AlGaN UVB LED grown on an AlN template. Japanese Journal of Applied Physics, 2019, 58, SAAF01.	1.5	27
20	Recent Progress Toward Realizing AlGaN-Based Deep-UV Laser Diodes. The Review of Laser Engineering, 2019, 47, 196.	0.0	3
21	Growth and characterization of low composition Ge, <i>x</i> in epi-Si _{1â⁻ <i>x</i>} Ge <i>x</i> (<i>x</i> ⩽  10%) active layer for fabrication of hydrogenated bottom so Journal Physics D: Applied Physics, 2018, 51, 185107.	ol a r&ell.	5
22	Physicochemical properties of the AC-excited helium discharges using a water electrode. Plasma Science and Technology, 2018, 20, 075403.	1.5	10
23	High photodetectivity of low-voltage flexible photodetectors assembled with hybrid aligned nanowire arrays. Journal of Materials Chemistry C, 2018, 6, 6510-6519.	5.5	23
24	In Vitro Cytotoxicity and Morphological Assessments of GO-ZnO against the MCF-7 Cells: Determination of Singlet Oxygen by Chemical Trapping. Nanomaterials, 2018, 8, 539.	4.1	25
25	Donor and acceptor levels in impurity-doped semiconducting BaSi ₂ thin films for solar-cell application. Physica Status Solidi (A) Applications and Materials Science, 2017, 214, 1700019.	1.8	10
26	Donor and acceptor energy levels in impurity Sb-, In-, Ag- and Cu-doped semiconducting BaSi2 thin films for device applications. Energy Procedia, 2017, 124, 612-620.	1.8	3
27	Development of wide band gap p-a-SiOxCy:H using additional trimethylboron as carbon source gas. Electronic Materials Letters, 2016, 12, 462-467.	2.2	7
28	Investigation of crystallinity and planar defects in the Si nanowires grown by vapor–liquid–solid mode using indium catalyst for solar cell applications. Japanese Journal of Applied Physics, 2016, 55, 01AE03.	1.5	7
29	Theoretical investigation about the optical characterization of coneâ€shaped pinâ€Si nanowire for top cell application. Energy Science and Engineering, 2016, 4, 383-393.	4.0	6
30	Control of verticality and (111) orientation of In-catalyzed silicon nanowires grown in the vapour–liquid–solid mode for nanoscale device applications. Journal of Materials Chemistry C, 2015, 3, 11577-11580.	5.5	10
31	Fabrication and characterization of BaSi ₂ epitaxial films over 1 µm in thickness on Si(111). Japanese Journal of Applied Physics, 2014, 53, 04ER04.	1.5	31
32	Engineering of p-n junction for high efficiency semiconducting BaSi2 based thin film solar cells. , 2014, , , .		0
33	Precipitation control and activation enhancement in boron-doped p <i>+</i> -BaSi2 films grown by molecular beam epitaxy. Applied Physics Letters, 2014, 104, .	3.3	32
34	Lattice and grain-boundary diffusions of boron atoms in BaSi2 epitaxial films on Si(111). Journal of Applied Physics, 2013, 113, .	2.5	21
35	<i>In-situ</i> heavily <i>p</i> -type doping of over 1020 cmâ^'3 in semiconducting BaSi2 thin films for solar cells applications. Applied Physics Letters, 2013, 102, .	3.3	72
36	Molecular beam epitaxy of boron doped p-type BaSi2 epitaxial films on Si(111) substrates for thin-film solar cells. Journal of Crystal Growth, 2013, 378, 201-204.	1.5	18

#	Article	IF	CITATIONS
37	Lattice and grain-boundary diffusions of impurity atoms in BaSi2 epitaxial layers grown by molecular beam epitaxy. Journal of Crystal Growth, 2013, 378, 189-192.	1.5	9
38	Enhanced p-type conductivity and band gap narrowing in heavily B-doped p-BaSi <inf>2</inf> films grown by molecular beam epitaxy. , 2013, , .		0
39	Fabrication and characterizations of phosphorusâ€doped nâ€ŧype BaSi ₂ epitaxial films grown by molecular beam epitaxy. Physica Status Solidi C: Current Topics in Solid State Physics, 2013, 10, 1753-1755.	0.8	15
40	Fabrication of n ⁺ â€BaSi ₂ /p ⁺ â€Si tunnel junction on Si(001) surface for characterization of photoresponse properties of BaSi ₂ epitaxial films. Physica Status Solidi C: Current Topics in Solid State Physics, 2013, 10, 1773-1776.	0.8	0
41	Effect of Solid-Phase-Epitaxy Si Layers on Suppression of Sb Diffusion from Sb-Doped n ⁺ -BaSi ₂ /p ⁺ -Si Tunnel Junction to Undoped BaSi ₂ Overlayers. Japanese Journal of Applied Physics, 2012, 51, 04DP01.	1.5	1
42	Molecular Beam Epitaxy of BaSi\$_{2}\$ Films with Grain Size over 4 \$mu\$m on Si(111). Japanese Journal of Applied Physics, 2012, 51, 098003.	1.5	18
43	Electrical characterization and conduction mechanism of impurity-doped BaSi2 films grown on Si(111) by molecular beam epitaxy. Thin Solid Films, 2012, 522, 95-99.	1.8	45
44	Improved internal quantum efficiency in high-quality BaSi <inf>2</inf> films grown by molecular beam epitaxy. , 2012, , .		0
45	Improved photoresponsivity of semiconducting BaSi ₂ epitaxial films grown on a tunnel junction for thin-film solar cells. Applied Physics Letters, 2012, 100, 152114.	3.3	50
46	Effect of Solid-Phase-Epitaxy Si Layers on Suppression of Sb Diffusion from Sb-Doped n ⁺ -BaSi ₂ /p ⁺ -Si Tunnel Junction to Undoped BaSi ₂ Overlayers. Japanese Journal of Applied Physics, 2012, 51, 04DP01.	1.5	1
47	Molecular Beam Epitaxy of BaSi2Films with Grain Size over 4 µm on Si(111). Japanese Journal of Applied Physics, 2012, 51, 098003.	1.5	2
48	Kinematic analysis of periodic continuous gaits for a bio-mimetic walking robot. , 2011, , .		4
49	Photoresponse properties of BaSi2 epitaxial films grown on the tunnel junction for high-efficiency thin-film solar cells. Thin Solid Films, 2011, 519, 8501-8504.	1.8	18
50	Al- and Cu-doped <mml:math <br="" altimg="si1.gif" xmlns:mml="http://www.w3.org/1998/Math/MathML">display="inline" overflow="scroll"> <mml:msub> <mml:mrow> <mml:mstyle mathvariant="normal"> <mml:mi> BaSi</mml:mi> </mml:mstyle </mml:mrow> <mml:mrow> <mml:mn>2films on Si(111) substrate by molecular beam epitaxy and evaluation of depth profiles of Al and Cu</mml:mn></mml:mrow></mml:msub></mml:math>	nn> ≰/₂ nml:	mr 2w >
51	atoms. Physics Procedia, 2011, 11, 11-14. Fabrication of BaSi2 films on transparent CaF2 (111) substrates by molecular beam epitaxy for optical characterization. Physics Procedia, 2011, 11, 189-192.	1.2	2
52	Modelling and Simulation of Flexibility Induced Disturbances for a Flying Rocket. IFAC Postprint Volumes IPPV / International Federation of Automatic Control, 2004, 37, 1015-1018.	0.4	0
53	Molecular Beam Epitaxy of Cu-Doped BaSi ₂ Films on Si(111) Substrate and Evaluation & Qualification of Depth Profiles of Cu Atoms for the Formation of Efficient Solar Cells. Advanced Materials Research, 0, 326, 139-143.	0.3	3
54	Indium (In)-Catalyzed Silicon Nanowires (Si NWs) Grown by the Vapor–Liquid–Solid (VLS) Mode for Nanoscale Device Applications. , 0, , .		0